TRANSIENT FINITE ELEMENT ANALYSIS OF INDUCTION MACHINES WITH STATOR WINDING TURN FAULT

B. Vaseghi, N. Takorabet, and F. Meibody-Tabar

Green Lab., CNRS (UMR 7037)
Nancy University, INPL, ENSEM
2, Avenue de la Forêt de Haye, Vandoeuvre-lès-Nancy, 54516, France

Abstract—In this paper, a time stepping two-dimensional FEM is performed for modeling and analysis of a IM with insulation failure inter-turn fault. FEM analysis is used for magnetic field calculation and the magnetic flux density and vector potential of machine is obtained for healthy and faulty cases. Comparing the magnetic flux distribution of healthy and faulty machines helps to detect the influence of turn fault. The machine parameters (self and mutual inductances) are obtained for IM with inter-turn fault. Finally, the FEM machine model is used for studying the machine under different fault condition. Study results including phases and fault currents express the behavior of machine with inter-turn faults. The symmetrical current components of IM with different fault severity are obtained by FE study and studied. The machine torque in healthy and faulty condition is also obtained and compared. The torque vibration increase upon to degree of fault.

1. INTRODUCTION

Induction machines (IM) are widely used in industry thanks to their low cost, reasonable size and low maintenance. For these applications high reliability is required. Therefore, predicting a coming fault by on-line health monitoring is helpful for increasing the system reliability. Fault detection and diagnosis leads to predict of coming fault in the electrical machine drive system by observing the deviation in parameters and behavior. Furthermore, it is also possible to predict the fault location. The results of fault studies help the machine designers to improve the fault tolerance as well the overall design of the machine drive system.

Corresponding author: B. Vaseghi (babak_vaseghi@yahoo.com).

One of the most common faults in the electrical motors is the inter-turn short circuit in the one of the stator coils. The increased heat due to this short circuit may also lead to turn-turn and turn to ground faults. The inter-turn fault is mostly caused by mechanical stress, moisture and partial discharge, which is accelerated for electrical machines supplied by inverters [1, 2].

Modeling, study and determining the parameters of electrical machine with insulation inter-turn fault is first step in the development of fault diagnosis and fault tolerant machine design. These models exhibit a trade-off between simplicity and precision. Study of transient and steady-state behavior of electrical machines under fault conditions by these fault models enable correct evaluation of measured data of diagnostic techniques [3–8]. Fault study of electrical machines can be operated either by physical experiments or computer-based analysis. Obviously, studying fault in electrical machine by computer based simulation is preferred because of economical, flexibility and safety problems.

The most used methods for modeling and detection of faults in electrical machines are: Winding function method (WFM), dynamic circuit base method (DCM) and finite element method (FEM).

The winding function based method uses motor geometrical parameters and does not take to account the core saturation [9–16]. The dynamic circuit based methods uses the generalized theory of electrical machines incorporating qdo axis. The same transformation process is applied in asymmetrical induction motors [17–21]. The circuit based model uses linearized magnetic parameters in fault analysis and detection and therefore, is not very precise and accurate. However, this method is faster and takes shorter time for computation. Finite Element Method (FEM) can be used for machine modeling especially under fault conditions. FEM gives much more precise information of the machine than other analytical analysis, which uses magnetic linearized parameters. FEM is based on magnetic field calculation using machine geometry dimensions and materials. By calculation of magnetic field distribution, the machine parameters such as magnetic flux density, inductances and electromagnetic torques can be obtained. FEM is capable to consider the magnetic field saturation effect based on motor performance. It also considers the spatial harmonic effects, split winding pattern and non-linear ferromagnetic materials in electrical machines [22–29]. Therefore, it can be applied in modeling and analysis of electrical machines with fault and unbalanced cases. The study of electrical machines in steady state, transient and fault conditions requires accurate knowledge of the equivalent circuit parameters. Furthermore, when a fault occurs the current and flux

density distribution is more or less modified as a function of fault severity. Therefore, it is necessary to study the electromagnetic flux and machine parameters for machine under stator and rotor faults.

Finite Element Method (FEM) is widely used for electrical machine model and parameter identification especially under different fault conditions. In [19, 20, 30, 31] the stator inter-turn fault of electrical machines is studied and analyzed by time stepping FEM. In [32, 33], FEM is used to analysis the induction motor with rotor broken bars. The magnetic field is obtained for healthy and faulty machine and compared.

Time stepping finite element coupled circuit method is capable to study the transient performance of electrical machines. Previously, the steady state analysis of electrical machines was applied, but thank to the availability of powerful computers the transient FE analysis of electrical machines can be carried out by applying time stepping coupled circuit method.

In this paper, a time stepping two-dimensional FEM is performed for modeling analysis of a IM with insulation failure inter-turn fault using Flux-2D software [34]. The turn fault in stator winding is considered in 25% of one phase winding. The insulation fault resistance is varied from 50 to 1 ohm. FEM analysis is used for magnetic field calculation and the magnetic flux density and vector potential of machine is obtained and analyzed for healthy and faulty cases. Comparing the magnetic flux distribution of healthy and faulty machines helps to detect the influence of turn fault. The machine parameters (self and mutual inductances) are obtained for IM with inter-turn fault. Finally, the FEM machine model is used for studying the machine under different fault condition. Study results including phases and fault currents express the behavior of machine with inter-turn faults. The symmetrical current components of IM with different fault severity are obtained by FE study and studied. The machine torque in healthy and faulty condition is also obtained and compared. The torque vibration increase upon to degree of fault.

2. FEM IM INTER-TURN FAULT MODEL AND FIELD STUDY

An inter-turn fault denotes an insulation failure between two windings in the same phase of the stator. The insulation failure is modeled by a resistance, where its value depends on the fault severity. The stator winding of a IM machine with inter-turn fault is represented in Fig. 1. In this figure, the fault is occurred in the phase a_s and r_f represents the fault insulation resistance. The subwindings (a_{s_1})
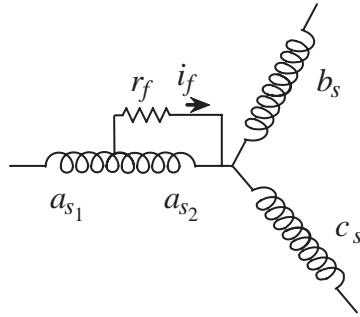
Figure 1. Stator circuit of IM with inter-turn fault in the phase as.

and (a_{s_2}) represent the healthy and faulty part of the phase winding a respectively. When fault resistance (r_f) decreases toward zero, the insulation fault evaluates toward an inter-turn full short-circuit. The evolution between $r_f = \infty$ and $r_f = 0$ is very fast in most insulation materials.

The physical systems are frequently represented by partial differential equations (PDE) system associated to boundary conditions in space and time. FEM allows a discrete representation of these non-linear equations converting them into an algebraic equations system. If the magnetic field is time-varying, eddy currents can be induced in materials with non-zero conductivity. Therefore, the time-varying field equation can be used for modeling the IM which has eddy current.

The Maxwell flux equation for time-harmonic magnetic problems is given as below:

$$\nabla \times \left(\frac{1}{\mu} \nabla \times A \right) = J - \sigma \partial_t A \qquad (1)$$

where $A \, (\mathrm{Wb/m})$ is the magnetic vector potential, $J \, (\mathrm{A/m^2})$ is the total current density vector, $\mu \, (\mathrm{H/m})$ is the magnetic permeability and $\sigma \, (\mathrm{S/m})$ is the electric conductivity. The current density vector J and the magnetic vector potential A are normal to the two dimensional (x, y) plane and the flux density vector B has components only in the (x, y) plane:

$$J = (0, 0, J_Z), \quad A = (0, 0, A_z), \quad B = (B_x, B_y, 0). \qquad (2)$$

When the oscillating frequency is fixed, we will have the exponential form for vector potential A as below:

$$A = |A_z| e^{j(\omega t)} \qquad (3)$$

with $\omega = \omega_r = 2\pi f_r$. ($\omega_r$ is the source electrical frequency).

Thus, with constant magnetic permeability μ, the field problem (1) is described by differential equation:

$$\frac{1}{\mu}\left(\frac{\partial^2 A_z}{\partial x^2} + \frac{\partial^2 A_z}{\partial y^2}\right) = j - \sigma j \omega_r A \qquad (4)$$

In this way, a two-dimensional analysis is carried out, yielding to shorter computation time and field solutions are more easily interpreted. The 3D effects are particularly important in determining the IM performances. They are due to finite axial length, stator end-windings and rotor rings, as well as the rotor slot skewing. The 3D effects are considered including appropriate elements in the equivalent circuit which are external to the field solution. In 2D FEM analysis, it is necessary to take into account the end-winding leakages for an adequate definition of the coupled circuit [35]. In this research, the 3D effects such as stator end winding and rotor ring equivalent parameters are calculated and included in electrical coupled circuit. The computation time of analysis can be reduced by applying the geometrical symmetry in machine geometry and boundary conditions. That means one part of machine is modeled and the magnetic field calculation is extended to whole part of geometry. It must be noted that this technique can not be used for study a machine with fault because the fault will be considered in whole part of machine by applying symmetry in electrical machine modeling.

For pre-processing stage of FEM analysis, the geometrical model, physical material properties, mesh generation are required. The boundary conditions have to be set up with geometrical model. For transient analysis the electrical coupled circuit is essential part of FEM analysis. A rotating air gap is considered in the machine geometry.

The two dimensional flux calculations are performed for study and analysis the IM with stator winding turn fault. Fig. 2 shows the mesh generation of the studied three-phase squirrel cage IM. The generated
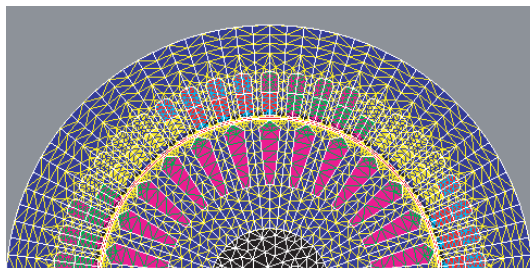
Figure 2. Cross section and mesh generation the studied IM.
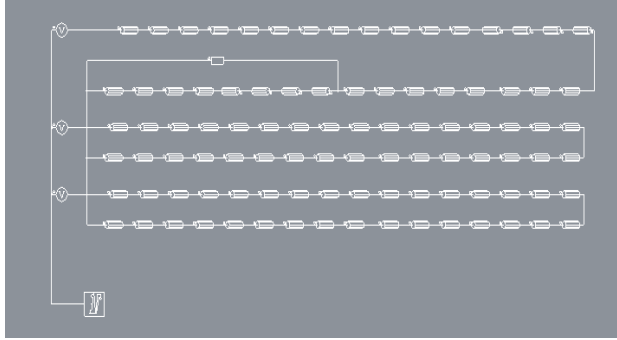
Figure 3. Coupled electrical circuit for transient FE analysis of IM machine.

mesh nodes number is 25420. The mesh elements are smaller in the air gap and regions close to it.

The electrical coupled circuit for transient analysis is shown in Fig. 3. The electric sources and unknown machine parameters are coupled with the FEM field equations. The FEM electromagnetic field equations are related to the coupled external circuit as follows:

$$
[K \quad C] \begin{bmatrix} A \\ i \end{bmatrix} + [Q \quad R] \begin{bmatrix} \dfrac{\partial A}{\partial t} \\ \dfrac{\partial i}{\partial t} \end{bmatrix} = P
\tag{5}
$$

where $[K]$, $[C]$, $[Q]$ and $[R]$ are the coefficient matrices and the vector P depends on input voltage. The magnetic vector potential $[A]$ and phase stator currents $[i]$ is determined must be obtained from (5). For the steady-state operation of machine the Equation (5) simplifies to:

$$
[K \quad C] \begin{bmatrix} A \\ i \end{bmatrix} + [Q \quad R] \begin{bmatrix} j\omega A \\ j\omega I \end{bmatrix} = P
\tag{6}
$$

The solution of the field problem consists of the knowledge of the magnetic vector potential in the field domain. The flux density is derived from vector potential. Determining the magnetic vector potential from (5) and (6), the magnetic flux density can be obtained as:

$$
B = \nabla \times A
\tag{7}
$$

The flux lines are the lines to which the flux density is parallel. They correspond to the equipotential lines of the magnet vector potential.

The instantaneous joule power losses are given by:

$$P_j = \int \rho \frac{|J_z|^2}{2} dt \qquad (8)$$

The stored magnetic energy in the structure can be computed as:

$$W_m = \frac{1}{2} \iint H \, dB \, dt = \iint J \, dA \, dt \qquad (9)$$

The tangential and normal components of the magnetic force (F_t, F_n) can be calculated via the method of Maxwell stress tensors as:

$$F_t = \frac{1}{\mu_o} B_n B_t$$
$$F_n = \frac{1}{2\mu_o} (B_n^2 - B_t^2) \qquad (10)$$

where B_n and B_t are the tangential and normal components of the magnetic flux density. The electromagnetic torque is calculated as:

$$T_{em} = \frac{rl}{\mu_o} \oint B_n B_t ds \qquad (11)$$

Finite element method is used for field calculation of healthy and faulty machine using [34] which is suitable for these applications. The simulation time was set up to $150 \, (\text{ms})$ with the step time equal to $0.5 \, (\text{ms})$. The machine is in full load operation and supplied by a voltage source with the amplitude of $50 \, (\text{V})$. Machine parameters are
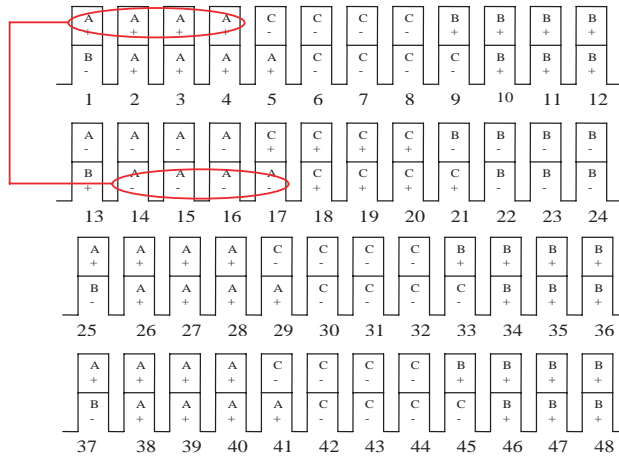
Figure 4. Winding diagram of the studied IM.

listed in Table 1. The studied IM has 48 slots and 4 poles with double layer stator winding. The winding diagram of the studied IM is illustrated in Fig. 4. To perform the inter-turn fault, the winding where the fault occurs, is divided into two portions which are linked to 2 sub-windings connected in series (a_{s_1}, a_{s_2}). With such a procedure, the magnetic flux linked with each winding branch is accessible. In the coupled electrical circuit the fault part of phase winding is short-circuited with a fault insulation resistance.

The fraction of faulty turns in stator winding inter-turn fault is considered 25% of phase *as* winding. The magnetic flux distribution of healthy and faulty IM at $t = 0.4$ (s) is shown in Fig. 5. It is seen that the flux distribution is symmetrical in the case of healthy machine while it becomes asymmetrical for the machine with inter-turn fault. It is seen that the path and polarity of flux is changed near faulty slot windings. Comparing the magnetic flux distribution of healthy and faulty machines helps to detect the influence of turn fault. The deviation of flux distribution leads to vibration torque; noise and un-unified magnetic stress depend on the fault severity.

(a)   (b)
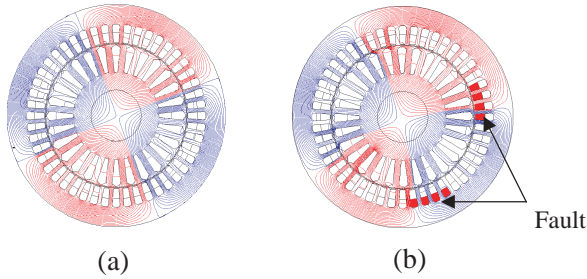
Figure 5. IM flux distribution at $t = 0.4$ s (a) healthy machine, (b) faulty machine.
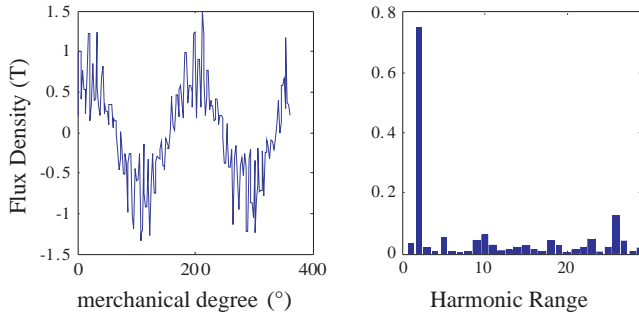
Figure 6. Flux density and its harmonics in healthy machine.
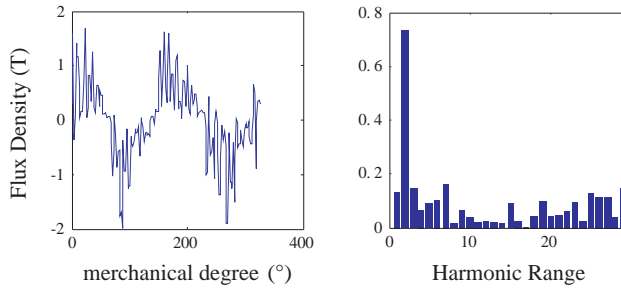
Figure 7. Flux density and its harmonics in faulty machine.
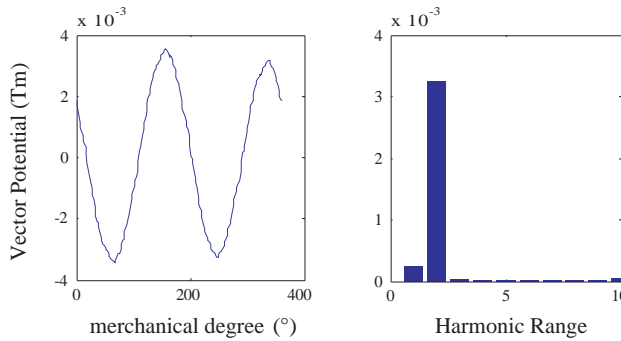
Figure 8. Vector potential and its harmonics in healthy machine.
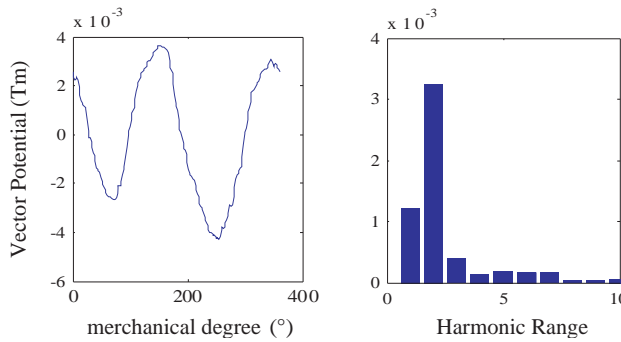
Figure 9. Vector potential and its harmonics in healthy machine.

The radial flux density in the air gap (B) for the healthy and faulty IM with their harmonics are calculated and presented in Figs. 6 and 7. It can be observed that flux density and vector potential of the machine with inter-turn fault becomes less sinusoidal and

unsymmetrical. The harmonic magnitude of the machine is increased after occurring inter-turn fault. As the turn fault degree increase, the magnetic field distribution is more asymmetrical and contains more harmonic components. The odd harmonics of magnetic flux density produce the principal of MMF in air gap and even harmonics of magnetic flux density produce the ripples of MMF in air gap.

The harmonics of electromagnetic flux is more visible in the vector potential variable. Thus, the vector potential over air gap is obtained by FEM. Figs. 8, 9 shows the calculated vector potential and its harmonic for healthy and faulty machine. It is seen that in the case of faulty machine, the vector potential is more asymmetrical and harmonic components is increased significantly.

Therefore, the stator turn fault in induction machines yields to magnetic field disturbance and deviation to healthy case which produce the torque fluctuation, noise and asymmetrical machine. The detection of fault can be carried out by observing the external values such as: currents, torque, and power.

Because of asymmetry flux distribution in faulty machine (Figs. 5–9), using linearized parameters in dynamic fault model for studying the machine with fault is not very precise. The accurate parameters for dynamic fault model can be calculated by FEM analysis.

By calculating the electromagnetic flux based on FEM, the machine inductances can be obtained. The machine inductances are calculated under fault condition when the inter-turn fault is occurred over 25% of turn numbers of the whole phase a_s winding. The self and mutual inductances of the healthy and faulty machine are calculated by FEM analysis. In order to calculate the self and mutual inductances of IM, the electrical circuit is supplied in only one winding and then the flux linkage for each bobbin is calculated at synchronous speed (there is no induced current at synchronous speed). Then, the calculated flux is divided by the current that is produced the flux, for example we have: and listed in Table 1.

$$L_{a_1} = \frac{\psi_{a_1}}{i_{a_1}}\Big|_{i_{a_2,\,b,\,c}} = 0, \quad M_{a_1 a_2} = \frac{\psi_{a_2}}{i_{a_1}}\Big|_{i_{a_2,\,b,\,c}} = 0$$

$$L_{a_2} = \frac{\psi_{a_2}}{i_{a_2}}\Big|_{i_{a_1,\,b,\,c}} = 0, \quad M_{a_2 b} = \frac{\psi_b}{i_{a_2}}\Big|_{i_{a_1,\,b,\,c}} = 0 \tag{12}$$

The machine parameters (self and mutual inductances) in healthy and faulty condition are obtained by field study and presented in Table 1. where L_{a_1} and L_{a_2} are the self-inductance of the healthy and faulty parts of phase a_s winding (a_{s_1}, a_{s_2}). $M_{a_1 b}$ and $M_{a_1 c}$ are mutual inductances between a_{s_1} and the windings b_s and c_s. In addition, $M_{a_1 a_2}$, $M_{a_2 b}$ and $M_{a_2 c}$ are respectively the mutual inductances between a_{s_2} and the windings a_{s_1}, b_s and c_s (Fig. 1).

Table 1. Studied IM inductances calculated by FEM in (mH). (a) Without fault. (b) With fault.

L_a	M_{ab}	M_{ac}
104.6	-52	-52

(a)

L_{a_1}	L_{a_2}	$M_{a_1 a_2}$	$M_{a_1 b} = M_{a_1 c}$	$M_{a_2 b} = M_{a_2 c}$
67.5	16	10.5	-37.5	-15

(b)

Table 2. Machine parameters.

Description	Value
Number of Poles	4
Winding turn No./Slot	$2*19$
Supply Frequency	$50\,\text{Hz}$
Supply Voltage	$380\,\text{V}$
Stator Inductance	$104\,\text{mH}$
Stator Resistance	$2\,\Omega$
Rotor Resistance	$0.4\,\Omega$
Power Factor	0.86
Inertia	$0.14\ \text{kg·m}^2$
Efficiency	84%
Slip Speed	4%
Rated Torque	$37\,\text{N·m}$
Rated Power	$5.5\,\text{kW}$

3. INTER-TURN FAULT STUDY RESULTS

Two dimensional time-stepping FEM analysis with external coupled circuit has been used to study the behavior of IM under different inter-turn winding fault conditions. Machine parameters are listed in Table 2. The machine is supposed to be supplied by a 3-phase sinusoidal voltage source ($50\,\text{V}, 50\,\text{Hz}$). In this paper, for study the inter-turn fault, the fault insulation resistance and the fault turn numbers are varied and the results are discussed (Fig. 10).
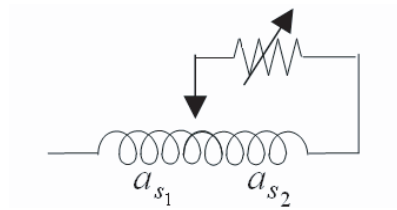
Figure 10. Schematics of fault study.
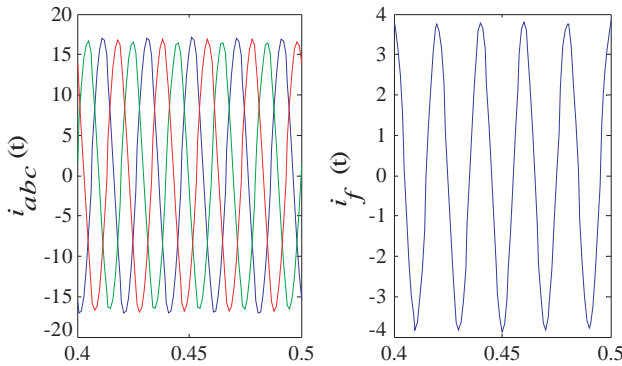
Figure 11. Fault study result for $r_f = 20$ ohm.
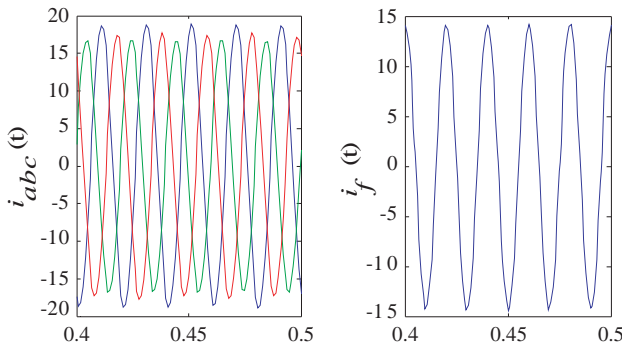
Figure 12. Fault study result for $r_f = 5$ ohm.

In the first case, the fraction of shorted turns is considered to be 25% of the phase as winding. Then, for two different values of fault insulation resistance: $r_f = 20\,\Omega$ and $r_f = 5\,\Omega$, the phase currents (i_{abc}) and the fault current (i_f) are obtained by FE analysis and presented in Figs. 11, 12. It is observed that when the fault resistance decreases,

the fault current and phase currents amplitudes increase and the phase currents become more and more unbalanced and non-sinusoidal. The asymmetry in magnetic field distribution leads to more phase current harmonics. The current of the faulty phase (a_s) is higher compared to the currents of the other healthy phases $(b_s$ and $c_s)$.

The electromagnetic torque of the IM under inter-turn fault over 25% of phase as winding and fault resistance $1\,\Omega$ is shown in Fig. 13. As it is mentioned, due to asymmetrical field distribution and nonsinusoidal phase currents, the torque ripple increases in faulty condition depend on fault degree.

Then, for studying the inter-turn fault severity, the value of the insulation fault resistance is varied between $100\,\Omega$ and $2\,\Omega$. The fault FEM model of IM is used to study the fault results for each fault resistance. The fault current profile for these fault resistances of FEM model and experimental test is shown in Fig. 11. For more clarity the logarithm of fault insulation resistances is used in Fig. 14.

The symmetric components (I_{PN}) and the spectral harmonics (I_h) of the phases currents for different fault resistances are calculated as follows:

$$I_{abc,\,h} = (1/T) \int_T i_{abc,\,h}(t) \exp(j2\pi ht/T)dt \qquad (13)$$
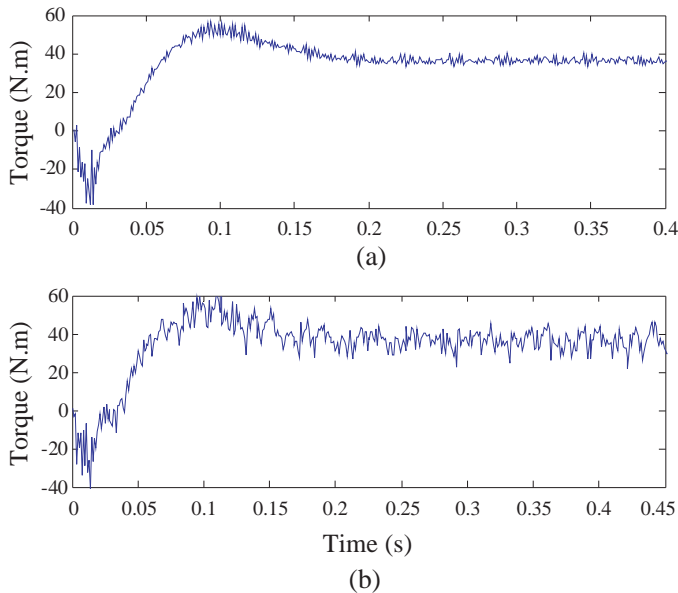
Figure 13. Torque of IM (a) healthy machine, (b) faulty machine.

$$\begin{bmatrix} I_P \\ I_N \end{bmatrix} = \begin{bmatrix} 1 & -\frac{1}{2} - j\frac{\sqrt{3}}{2} & -\frac{1}{2} + j\frac{\sqrt{3}}{2} \\ 1 & -\frac{1}{2} + j\frac{\sqrt{3}}{2} & -\frac{1}{2} - j\frac{\sqrt{3}}{2} \end{bmatrix} \begin{bmatrix} I_a \\ I_b \\ I_c \end{bmatrix} \qquad (14)$$

The symmetric components and the harmonic components of the stator phases currents versus the log of fault resistance variations are shown in Fig. 15.
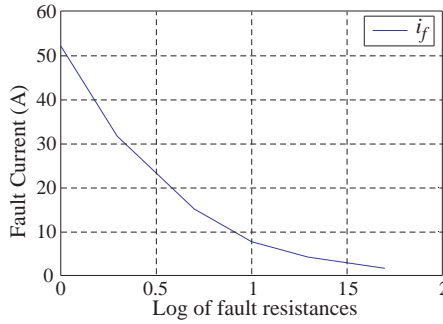
Figure 14. Fault current versus logarithm of different fault resistances.
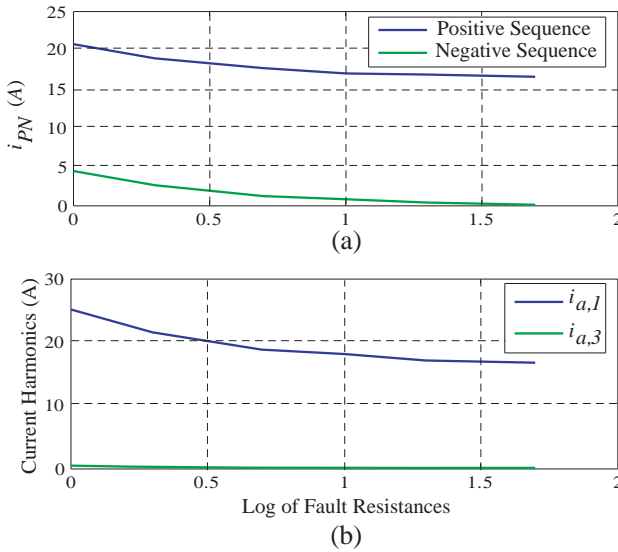
Figure 15. Phases current symmetrical components and harmonics versus log. of fault resistance.

From Figs. 14 and 15, it can be revealed that, as the fault resistance decrease, the fault current and the phases currents harmonics and symmetric components will increase. The 3rd harmonic is very small comparing to main harmonic. It can be seen that from less than $R_f < 3\,\Omega$ or $(\text{Log}(R_f) < 0.5)$, the negative sequence is significant and reaches to about 30% of the positive sequence.

Therefore in this research, using two dimensional time stepping Finite element method, the IM under various stator inter-turn fault conditions is studied. The fault study results for different fault severity and locations are obtained and analyzed. These results can be helpful for electrical machine designers in the aspect of fault tolerant machines. Also, it can be useful for fault diagnosis monitoring systems.

4. CONCLUSION

In this paper, a time stepping two-dimensional FEM is performed for modeling and analysis of a IM with insulation failure inter-turn fault. FEM analysis is used for magnetic field calculation and the magnetic flux density and vector potential of machine is obtained for healthy and faulty cases. Comparing the magnetic flux distribution of healthy and faulty machines helps to detect the influence of turn fault. The machine parameters (self and mutual inductances) are obtained for IM with inter-turn fault. Finally, the FEM machine model is used for studying the machine under different fault condition. Study results including phases and fault currents express the behavior of machine with inter-turn faults. The symmetrical current components of IM with different fault severity are obtained by FE study and studied. The machine torque in healthy and faulty condition is also obtained and compared. The torque vibration increase upon to degree of fault.

The results of this research are expected to help the machine designers to improve the fault tolerance aspect as well the overall design of the machine drive system.

REFERENCES

1. Kliman, G. B., W. J. Premerlani, R. Kogel, and D. Howeler, "A new approach to on-line turn fault detection in AC motors," *IEEE Industry Application Conference*, IAS, 1996.
2. Thomson, W. T., "A review of on-line condition monitoring techniques for three-phase squirrelcage induction motors — Past present and future," *IEEE International Symposium on Diagnostics for Electrical Machines, Power Electronics and Drives*, 1999.

3. Cusido, J., L. Romeral, J. A. Ortega, J. A. Rosero, and A. Garcia Espinosa, "Fault detection in induction machines using power spectral density in wavelet decomposition," *IEEE Transactions on Industrial Electronics*, Vol. 55, No. 2, 633–643, Feb. 2008.

4. Akin, B., U. Orguner, H. A. Toliyat, and M. Rayner, "Low order PWM inverter harmonics contributions to the inverter-Fed induction machine fault diagnosis," *IEEE Transactions on Industrial Electronics*, Vol. 55, No. 2, 610–619, Feb. 2008.

5. Zidani, F., D. Diallo, M. E. H. Benbouzid, and R. Nait-Said, "A fuzzy-based approach for the diagnosis of fault modes in a voltage-fed PWM inverter induction motor drive," *IEEE Transactions on Industrial Electronics*, Vol. 55, No. 2, 586–593, Feb. 2008.

6. Cruz, S. M. and A. Cardoso, "Stator fault diagnosis in three-phase synchronous and asynchronous motors," *IEEE Transaction on Industrial Applications*, Vol. 37, No. 5, 2001.

7. Lee, S.-B., R. M. Tallam, and T. G. Habetler, "A robust on-line turn-fault detection technique for induction machines based on monitoring the sequence component impedance matrix," *IEEE Transaction on Power Electronics*, Vol. 18, No. 3, 2003.

8. Toliyat, H. A. and T. A. Lipo, "Transient analysis of cage induction machines under stator, rotor bar end-ring faults," *IEEE Trans. Energy Conversion*, 241–247, 1995.

9. Luo, X., Y. Liao, H. A. Toliyat, and T. A. Lipo, "Multiple coupled circuit modelling of induction machines," *IEEE Transaction on Industrial Applications*, Vol. 31, No. 2, 311–317, 1995.

10. Toliyat, H. A. and T. A. Lipo, "Transient analysis of cage induction machines under stator, rotor bar end-ring faults," *IEEE Trans. Energy Conversion*, Vol. 10, No. 2, 241–247, 1995.

11. Joksimovic, G. M. and J. Penman, "The detection of inter-turn short circuits in the stator windings of operating motors," *IEEE Transactions on Industrial Electronics*, Vol. 47, No. 5, 1078–1084, 2000.

12. Sahraoui, M., A. Ghoggal, S. E. Zouzou, A. Aboubou, and H. Razik, "Modelling and detection of inter-turn short circuits in stator windings of induction motor," *IEEE Industrial Electronics, IECON*, 2006.

13. Faiz, J., I. Tabatabaei, and H. A. Toliyat, "An evaluation of inductances of a squirrel-cage induction motor under mixed eccentric conditions," *IEEE Trans. Energy Conversion*, Vol. 18, No. 2, 252–258.

14. Faiz, J. and I. Tabatabaei, "Extension of winding function theory for non uniform air gap in electric machinery," *IEEE Transactions on Magnetics*, Vol. 38, No. 6, 3654–3657, Nov. 2002.

15. Nandi, S., R. M. Bharadwaj, and H. A. Toliyat, "Performance analysis of a three-phase induction motor under mixed eccentricity condition," *IEEE Trans. Energy Conversion*, Vol. 17, No. 3, 392–397, Sep. 2002.

16. Nandi, S., S. Ahmed, and H. A. Toliyat, "Detection of rotor slot and other eccentricity related harmonics in a three phase induction motor with different rotor cages," *IEEE Trans. Energy Conversion*, Vol. 16, No. 3, 253–260, Sep. 2001.

17. Arkan, M., D. Kostic-Perovic, and P. J. Unsworth, "Modelling and simulation of induction motors with inter-turn faults for diagnostics," *ELSEVIER Journal of Electric Power System Research*, Vol. 75, No. 1, 57–66, 2005.

18. Bachir, S., S. Tnani, J.-C. Trigeassou, and G. Champenois, "Diagnosis by parameter estimation of stator and rotor faults occurring in induction machines," *IEEE Transactions on Industrial Electronics*, Vol. 53, No. 3, 963–973, 2006.

19. Vaseghi, B., B. Nahid-Mobarakeh, N. Takorabet, and F. Meibody-Tabar, "Modelling of non-salient PM synchronous machines under stator winding inter-turn fault condition: Dynamic model-FEM model," *Proc. IEEE VPPC*, 2007.

20. Vaseghi, B., N. Takorabet, and F. Meibody-Tabar, "Modeling of IM with stator winding interturn fault validated by FEM," *Proc. IEEE ICEM*, 2008.

21. Tallam, R. M., T. G. Habetler, and R. G. Harley, "Transient model for induction machines with stator winding turn faults," *IEEE Transaction on Industrial Applications*, Vol. 38, No. 3, 2002.

22. Williamson, S., L. H. Lim, and A. C. Smith, "Transient analysis of cage induction motor using finite elements," *IEEE Transactions on Magnetics*, Vol. 26, No. 2, 941–944, Mar. 1990.

23. Thorsen, O. V. and M. Dalva, "Failure identification and analysis for high voltage induction motors in petrochemical industry," *IEEE Transactions on Industrial Electronics*, Vol. 12, No. 2, 1998.

24. Tenhunen, A., T. Bendetti, T. P. Holopainen, and A. Arkkio, "Electromagnetic forces of the cage rotor in conical whirling motion," *IEE Proc. — Electr. Power Appli.*, Vol. 150, No. 5, 563–568, Sep. 2003.

25. Tenhunen, A., T. P. Holopainen, and A. Arkkio, "Effects of saturation on the forces in induction motors with whirling cage

rotor," *IEEE Transactions on Magnetics*, Vol. 40, No. 2, 766–769, Mar. 2004.

26. Tenhunen, A., "Calculation of eccentricity harmonics of the airgap flux density in induction machine by impulse method," *IEEE Transactions on Magnetics*, Vol. 41, No. 5, 1904–1907, May 2005.

27. Pham, T. H., P. F. Wendling, S. J. Salon, and H. Acikgoz, "Transient finite element analysis of an induction motor with external circuit connections and electromechanical coupling," *IEEE Trans. Energy Conversion*, Vol. 14, No. 4, 1407–1412, Dec. 1999.

28. Jian, L. and K.-T. Chau, "Analytical calculation of magnetic field distribution in coaxial magnetic gears," *Progress In Electromagnetics Research*, PIER 92, 1–16, 2009.

29. Watson, J. F., N. C. Paterson, and D. G. Dorrel, "Use of finite element methods to improve techniques for the early detection of faults in induction motors," *IEEE Trans. Energy Conversion*, Vol. 14, No. 3, 655–660, 1999.

30. Dai, M., A. Keyhani, and T. Sebastian, "Fault analysis of a PM brushless DC motor using finite element method," *IEEE Trans. Energy Conversion*, Vol. 20, No. 1, 2005.

31. Mohammad, O. A., Z. Liu, S. Liu, and N. Y. Abed, "Internal Short circuit fault diagnosis for PM machines using FE-based phase variable model and wavelets analysis," *IEEE Transactions on Magnetics*, Vol. 33, No. 4, 2007.

32. Faiz, J. and B. M. Ebrahimi, "Mixed fault diagnosis in three-phase squirrel-cage induction motor using analysis of air-gap magnetic field," *Progress In Electromagnetics Research*, PIER 64, 239–255, 2006.

33. Faiz, J., B. M. Ebrahimi, and M. B. B. Sharifian, "Time stepping finite element analysis of broken bars fault in a three-phase squirrel-cage induction motor," *Progress In Electromagnetics Research*, PIER 68, 53–70, 2007.

34. FLUX 2D, "CAD package for electromagnetic and thermal analysis using finite element," CEDRAT, Version 9.20, 2005.

35. Bianchi, N., *Electrical Machine Analysis Using Finite Elements*, Taylor & Francis, 2005.